Antihydrogen Production in a Paul Trap

G. Geyer * and R. Blümel †

Department of Physics, Wesleyan University,

Middletown, Connecticut 06459-0155

(Dated: August 8, 2011)

Abstract

Although positrons and antiprotons have vastly different masses, we show that it is possible to store both particle species simultaneously in a Paul trap, using the space charge of the positron cloud as a trap for the antiprotons. Computer simulations confirm the validity of this new trapping mechanism. In addition, the simulations show transient antihydrogen production that manifests itself in the intermittent production of bound positron-antiproton Rydberg states. Since realistic trapping parameters are used in the simulations, (i) simultaneous positron-antiproton trapping and (ii) transient antihydrogen formation should be experimentally observable in a Paul trap. Strategies are suggested to lengthen the lifetime of antihydrogen in the Paul trap.

PACS numbers: 37.10.Ty

* email: ggeyer@wesleyan.edu

† email: rblumel@wesleyan.edu

I. INTRODUCTION

Motivation for the production of antihydrogen ($\bar{\mathrm{H}}$) is drawn from the following three main goals:

1. Spectroscopy of its energy levels to confirm the hypothesis that antihydrogen has the same spectrum as hydrogen.

2. Testing the effects of a gravitational field on antimatter.

3. Serving as a first step towards the storage of antimatter for efficient rocket propulsion.

The first item above constitutes a rigorous test of the Charge Conjugation-Parity-Time Reversal (CPT) invariance theorem [1], a fundamental element of the standard model of particle physics. The CPT theorem predicts that the spectra of atoms and anti-atoms should be exactly the same. Any difference in measured spectra of atoms and anti-atoms would be inconsistent with CPT invariance and would necessitate major revisions of the standard model.

The second item also has exciting implications for fundamental physics, since the weight of antimatter, i.e. the force it experiences in a gravitational field, has not yet been experimentally determined. Not even the sign of the gravitational force of antimatter is known. Although some authors argue that it should be the same as ordinary matter (see, e.g., [2, 3]), others argue that matter and antimatter should repel each other (see, e.g., [4]). Only direct experimentation on anti-atoms can resolve the dispute on the behavior of antimatter in a gravitational field. Indeed, within the framework of the AEGIS collaboration [5], e.g., such experiments are currently under way.

Regarding the last item, $\bar{\mathrm{H}}$ seems to be the most promising option for means of constructing the "perfect" matter-antimatter burning interstellar space ship [6] due its relative simplicity and neutrality.

In light of the discussed scientific and engineering impact that positive results on antimatter formation would have, it is no surprise that many groups have been engaged in research regarding the production of $\bar{\mathrm{H}}$ for many years. The ALPHA [7] and ATRAP [8, 9] collaborations have both been successful at detecting $\bar{\mathrm{H}}$ formation in different types of modified Penning traps. Recently, the ALPHA collaboration trapped $\bar{\mathrm{H}}$ for 1000 s [10]. Magnetic

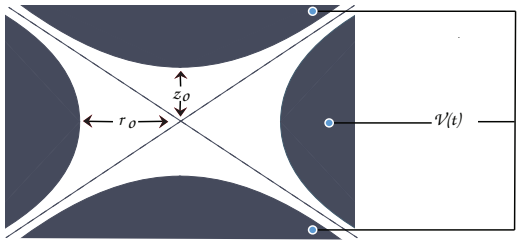

FIG. 1: Cross-sections of the three axially symmetric conducting hyperbolic electrodes of the Paul trap in the x-z plane. The two hyperbolas intersecting the z axis are the cross-sections of the two hyperbolic end-cap electrodes. The two hyperbolas on the left and on the right are the two cross-sections of the single, rotationally symmetric ring electrode of the trap. The two end caps are electrically connected. A superposition of a dc and an ac voltage, $V(t) = U_0 + V_0 \cos(\omega t)$, is applied between the end-cap electrodes and the ring electrode, where U_0 is the amplitude of the dc voltage and V_0, ω are the amplitude and frequency of the ac voltage, respectively. The distance of the end-cap electrodes from the center of the trap is z_0; the distance of the ring-electrode from the center of the trap is r_0.

traps, however, may not be optimal for the efficient formation of antimatter. Due to the Lorentz force, the magnetic fields impede the formation of neutral antimatter. In this paper, we investigate antimatter formation in an alternate trap that uses only electric fields: the Paul trap.

II. THEORETICAL BACKGROUND

A. Paul Trap Potential

The Paul trap [11] is a dynamical, charged-particle trap that consists of three conducting, axially symmetric, hyperbolic surfaces. The intersections of the three surfaces with the x-z plane are sketched in Fig. 1. As shown, two of the electrodes intersect the z axis and form the end-cap electrodes of the trap, while the third electrode is a hyperbolic, enclosing ring electrode. As shown in Fig. 1, a superposition

$$V(t) = U_0 + V_0 \cos(\omega t) \tag{1}$$

of a static (dc) voltage U_0 and an alternating (ac) voltage with amplitude V_0 and frequency ω is applied between the end caps, which are electrically connected, and the ring electrode. The shape of the electrodes and their arrangement is chosen such that the applied ac voltage creates an effective potential minimum, located at the center of the trap. It is this minimum which is capable of trapping charged particles forever.

For the following derivations, we note that the frequency of the ac voltage (typically ranging from a few MHz to about a GHz) and the amplitude of the ac voltage (typically on the order of a few hundred V or less) are small enough so that we can neglect magnetic field effects and treat the Paul-trap problem as approximately quasi-electrostatic, where the electric fields and potentials are adiabatically (very slowly) changing in time. This follows the usual computational treatment of the Paul trap in the literature (see, e.g., [11–13]), where magnetic fields are not considered.

If we define cylindrical coordinates in the usual way, with the z axis along the axis of symmetry of the trap and the x and y axes defined accordingly, and if we define $r^2 = x^2 + y^2$, the axial symmetry of the trap results in a potential of the form:

$$\Phi(x, y, z; t) = A(t)r^2 + B(t)z^2 \ . \tag{2}$$

According to Maxwell's equations in free space,

$$\nabla^2 \Phi(x, y, z; t) = 0. \tag{3}$$

Using (2) in (3) yields

$$B(t) = -2A(t). \tag{4}$$

Thus, we have

$$\Phi(x, y, z; t) = A(t)(r^2 - 2z^2), \tag{5}$$

i.e. the potential, (2), has a hyperbolic shape that would not trap charged particles if A and B were time-independent, static coefficients. This is a consequence of Earnshaw's theorem [14], which states that an electrostatic potential satisfying (3) cannot have a potential minimum. However, since the trapping potential, (2), is due to an *alternating* electric field, the Paul trap potential can have a dynamic minimum without violating Earnshaw's theorem [11].

Taking the time-dependence of the trap into account, we can set the potential of the end-caps and ring electrode to be $-\Phi_0(t)$ and $\Phi_0(t)$ respectively (see Fig. 1). We also define

the distance from the center of the trap to the ring electrode to be r_0, and from the center to the polar end caps to be z_0 (again, see Fig. 1). Then, at the intersection point of the upper end-cap electrode with the z axis ($r = 0, z = z_0$), we have:

$$\begin{aligned} -\Phi_0(t) &= -2A(t)z_0^2 \\ \implies \quad A(t) &= \frac{\Phi_0(t)}{2z_0^2}. \end{aligned} \tag{6}$$

Similarly, at the point ($r = r_0, z = 0$) on the ring electrode, we have:

$$\begin{aligned} \Phi_0(t) &= A(t)r_0^2 \\ \implies \quad A(t) &= \frac{\Phi_0(t)}{r_0^2}. \end{aligned} \tag{7}$$

Requiring

$$r_0^2 = 2z_0^2, \tag{8}$$

equations (6) and (7) are consistent and the potential, (5), becomes:

$$\Phi(x, y, z; t) = \frac{\Phi_0(t)}{r_0^2}(r^2 - 2z^2). \tag{9}$$

Let us now compute the time dependence. Since the applied voltage, (1), is the potential difference between the end-cap electrodes and the ring electrode, we have:

$$\begin{aligned} \Phi_0(t) - (-\Phi_0(t)) &= U_0 + V_0 \cos(\omega t) \\ \implies \quad \Phi_0(t) &= \frac{U_0 + V_0 \cos(\omega t)}{2}. \end{aligned} \tag{10}$$

Thus, the full, time-dependent form of our desired potential is written:

$$\Phi(x, y, z; t) = \frac{U_0 + V_0 \cos(\omega t)}{2r_0^2}(r^2 - 2z^2). \tag{11}$$

B. Charged Particles in a Paul Trap

Now that we have the trapping potential, we are ready to describe the motion of a trapped particle with mass m and charge Q within the trap. Denoting the position vector of the particle by $\mathbf{r} = (x, y, z)$, using Newton's second law, $\mathbf{F} = m\ddot{\mathbf{r}}$, together with the fact that the force on a particle with charge Q is given by

$$\mathbf{F} = Q\mathbf{E} = -Q\nabla\Phi(\mathbf{r}; t), \tag{12}$$

we obtain:

$$m\frac{d^2\mathbf{r}}{dt^2} = -Q\frac{U_0 + V_0\cos(\omega t)}{r_0^2}\begin{pmatrix} x \\ y \\ -2z \end{pmatrix}. \tag{13}$$

We simplify this equation by defining the following dimensionless constants:

$$a = \frac{4QU_0}{m\omega^2 r_0^2}\ , \quad q = \frac{2QV_0}{m\omega^2 r_0^2}\ , \quad \text{and} \quad \tau = \frac{\omega t}{2}, \tag{14}$$

where τ is the dimensionless time. The two other constants, a and q, act as control parameters: they determine the stability of the system. Only certain pairs (a, q) will produce a potential minimum. This is easier to see once we simplify the equations of motion into a set of three uncoupled equations that have the form of Mathieu's Equations [15]:

$$\frac{d^2\mathbf{r}}{d\tau^2} + [a + 2q\cos(2\tau)]\begin{pmatrix} x \\ y \\ -2z \end{pmatrix} = 0. \tag{15}$$

These are the canonical equations used to describe the motion of a charged particle in a Paul trap [11]. A physical analogy for the motion of a particle satisfying this relation would be to consider a saddle-shaped plate on a spinning platform [11]. When the platform is not spinning, which is analogous to the voltage not alternating (but still applied), a small ball placed somewhere near the center (or anywhere else) will roll off the side. However, if the saddle is spinning at an appropriate angular speed, the ball will remain on the platform and undergo a confined motion with small "zig-zag" perturbations about some average trajectory. That small scale motion is called the micro-motion while the larger-scale, average motion is called the macro-motion [16]. In the classical picture, there is a direct analogy between this mechanical situation and charged particles in a Paul trap.

III. NUMERICAL SIMULATIONS

The Paul trap excels at trapping charged particles of a single species. However, in general, it is not as effective at simultaneously trapping particles of different species. Consider our case: Positrons and antiprotons have an equal magnitude of charge, but differ in mass by a factor of roughly 1836. The (a, q) pair for each of these particles will be accordingly different, so they cannot both be *independently* confined in a specifically tuned Paul trap. However,

due to the Coulomb force, this does not rule out the possibility of these two oppositely charged particles being *simultaneously* trapped. In other words, their motion is no longer determined by the Paul trap potential alone. As we will confirm below, this creates new possibilities for stable trapping. Our simulations demonstrate this new type of stability and allow us to determine the viability of $\bar{\mathrm{H}}$ production in a Paul trap. Since the particles simulated are in a highly excited, relatively hot cloud state, quantum effects are expected to be exceedingly small, so our simulations are entirely classical.

A. Coupled Equations of Motion

In order to simulate interacting particles in the trap, we add the Coulomb force to the single-particle equation, (15). For dimensionless equations that can be simulated on a computer, we introduce a convenient unit of length, $l_0 = 1\,\mu$m, and define the dimensionless Coulomb constant

$$\Gamma = \frac{e^2}{m\omega^2 \pi \epsilon_0 l_0^3}. \tag{16}$$

We consider a system of N positrons and N' antiprotons, and introduce (in units of l_0) the dimensionless position vectors $\mathbf{r}_i = (x_i, y_i, z_i)$ for positron number i, and $\mathbf{R}_k = (X_k, Y_k, Z_k)$ for antiproton number k. Then, the dimensionless equations of motion for positron number, $i = 1, \ldots, N$, are:

$$\frac{d^2\mathbf{r}_i}{d\tau^2} + [a + 2q\cos(2\tau)] \begin{pmatrix} x_i \\ y_i \\ -2z_i \end{pmatrix} = \Gamma \sum_{\substack{j=1 \\ j\neq i}}^{N} \frac{\mathbf{r}_i - \mathbf{r}_j}{|\mathbf{r}_i - \mathbf{r}_j|^3} - \Gamma \sum_{j'=1}^{N'} \frac{\mathbf{r}_i - \mathbf{R}_{j'}}{|\mathbf{r}_i - \mathbf{R}_{j'}|^3}, \tag{17}$$

and for antiproton number, $k = 1, \ldots, N'$, are:

$$\frac{d^2\mathbf{R}_k}{d\tau^2} - \frac{1}{\rho}[a + 2q\cos(2\tau)] \begin{pmatrix} X_k \\ Y_k \\ -2Z_k \end{pmatrix} = \frac{\Gamma}{\rho} \sum_{\substack{j'=1 \\ j'\neq k}}^{N'} \frac{\mathbf{R}_k - \mathbf{R}_{j'}}{|\mathbf{R}_k - \mathbf{R}_{j'}|^3} - \frac{\Gamma}{\rho} \sum_{j=1}^{N} \frac{\mathbf{R}_k - \mathbf{r}_j}{|\mathbf{R}_k - \mathbf{r}_j|^3}, \tag{18}$$

where $\rho = M/m$ is the ratio of the antiproton mass M and the positron mass m.

B. Trap and Initial Conditions

According to the theory of Mathieu equations [15], trapping is achieved for (a, q) pairs in *stability tongues* that are well-known and defined by certain nonlinear equations [15]. For our

simulations, we chose $a = 0$ and $q = 0.1$. This pair corresponds to a parameter combination in the fundamental stability tongue [15], and may be realized by choosing $U_0 = 0\,\mathrm{V}$ and $V_0 = 100\,\mathrm{V}$. We also chose the size of the trap to be $r_0 = 5\,\mathrm{mm}$. All of the above choices are motivated by similar parameters for Paul traps typically used in the lab (see, e.g., [12]). For positrons ($Q = e$, where e is the elementary charge) and this choice of trap parameters, we obtain $\omega = 2\pi \times 597\,\mathrm{MHz}$ from the definition of q in (14). The particles' initial conditions were generated at random, but confined to be within $10\,\mu\mathrm{m}$ of the center of the trap.

C. FORTRAN Implementation

The programming language of choice was FORTRAN. The main routine simulates the interaction between an arbitrary number N of positrons and N' of antiprotons, evolving the equations of motion (17) and (18) by making calls to a numerical integrator of our choice. We carefully investigated the Euler, Runge-Kutta, and Velocity Verlet algorithms [17]. However, these methods were found to be inefficient for our simulations due to the vast changes in magnitude of the spatial separation of particles. Since particles may be as far away as several tens of μm and may approach as closely as several nm, we found it prudent to employ an integrator for which large order changes in length-scale were not an issue.

The accuracy delivered by conventional numerical integration routines is determined predominantly by the size of the time step taken by the controlling program. This imposes a limit on the efficiency of our simulations, which we ran on a 2.1 GHz Intel Core 2 Duo processor. For example, when increasing the number of particles in our trap, we increase the number of coupled differential equations. To maintain the same degree of accuracy that we achieved for a fewer number of coupled equations, we require a smaller step size due to the smaller average separation between particles. Thus, integrators with a fixed step size will work, but become more and more inefficient as one increases the accuracy. In order to overcome this obstacle, we implemented a 4th order Runge-Kutta method with 5th order adaptive step-size control [17]. This algorithm allows specification of the required accuracy and the integrator adjusts the size of the time steps dynamically during the integration to ensure that the specified accuracy requirement is met.

In order to detect antihydrogen formation, we solve the two-body reduced-mass problem [18] for each positron-antiproton pair along their trajectories $\mathbf{r}_i(t)$, $\dot{\mathbf{r}}_i(t)$, $\mathbf{R}_k(t)$, and $\dot{\mathbf{R}}_k(t)$.

We compute the associated principal quantum number

$$n(t) = \sqrt{\frac{-R}{E(t)}}, \tag{19}$$

where $R = 13.6\,\mathrm{eV}$ is the hydrogen Rydberg constant and $E(t)$ is the *classical* energy of the equivalent reduced-mass particle determined from the numerical solutions of (17) and (18). It is important to realize that $n(t)$ is a sensitive enough function of $E(t)$ that approximating the mass of the antiproton as infinite is not sufficient—the correct, finite mass must be used. Of course, a principal quantum number according to (19) exists only for $E(t) < 0$. For $E(t) > 0$ the associated positron-antiproton pair is not in a mutual bound state, no antihydrogen has formed, and the corresponding pair is not considered at this particular time t. A plot of $n(t)$ versus time for any positrons orbiting a parent antiproton allows us to determine if antihydrogen has been produced. A plateau in $n(t)$ corresponds to a bound pair (formed antihydrogen). Our simulations show that $\bar{\mathrm{H}}$ is preferentially produced in high Rydberg states, i.e. $n(t)$ is large (typically on the order of $n(t) \approx 100$).

IV. RESULTS

Our earliest attempts consisted of a single positron and a single antiproton with initial positions within $10\,\mu$m of the center of the trap. Since the potential in the Paul trap is time-dependent, the energy of the particles is not conserved [18]. Thus, our working hypothesis was that antihydrogen could be formed via "field-assisted recombination". This process may be understood in analogy to the known process of three-body recombination, in which a third particle interacts with a particle pair. In doing so, the third particle removes enough energy and angular momentum to force the original particle pair into a bound state. In our envisioned field-assisted recombination process, the field itself would play the role of the third particle. To test this, we conducted simulations of a single particle of either species. Within times comparable to those that it took to synthesize Rydberg $\bar{\mathrm{H}}$ with other initial trap conditions, we did not find the field-assisted recombination effect sufficient to form antihydrogen. If this effect exists, it is either negligible, or a theoretical or computational demonstration requires a quantum mechanical approach. Another consideration is that the field near the center of the trap is very weak. It may be that the effect is proportional to cloud size: a larger cloud would require more particles to be interacting with the strongly

varying part of the field. However, for many particle clouds, the field-assisted recombination effect, if it exists, would be difficult to separate from N-body recombinations.

Next, we simulated a scenario that would perhaps be the most conducive to experimental implementation: injecting an antiproton into a cloud of positrons already confined close to the center of the trap, but not crystallized [12]. Even when the initial speed of the antiproton was made very small, the energy it gained upon entry into the positron cloud took a long time to dissipate on the time scale of our simulation, which corresponds to only about 0.5 ms. The dominant motion of the antiproton was an oscillation between its starting position in the trap and a position diametrically opposite. Despite the large-amplitude oscillations, there was still some interaction with the individual positrons. Due to inelastic collisions, we did see the oscillation amplitude of the antiproton decrease somewhat over time. While we did not observe antihydrogen production in this scenario, we did confirm a new trapping mechanism. Even with trapping parameters optimized for positron confinement, binding of the negatively charged antiprotons to the positively charged positron cloud leads to strong antiproton trapping. This is one of the central results of our research.

Based on the new space-charge trapping mechanism, we conjecture that if we were able to simulate the antiproton's motion until it dissipated enough energy by inelastic collisions with the trapped positrons, the antiproton will be trapped within the positron cloud. The antiproton-positron cloud system will always be focused into the center of the trap due to the positron-optimized trapping parameters. The conjectured energy dissipation is motivated by the fact that while, from a distance, the positron cloud looks like a uniform charge distribution, when an antiproton passes through the cloud and interacts with the individual positrons, it imparts kinetic energy to them. This process will heat up the positron cloud, but it allows the antiproton to come within range of recombination with a relatively small amount of kinetic energy.

With these results and ideas in mind, we proceeded to simulate a third scenario, where the antiproton was already cooled and bound within the positron cloud. We found that transient recombination of positrons and antiprotons into $\bar{\mathrm{H}}$ indeed occurs in the Paul trap. The two specific cases in which we observed $\bar{\mathrm{H}}$ formation consisted of 10 positrons and either 1 or 2 antiprotons. In Fig. 2, as an example, we show the principal quantum number $n(t)$ versus time for one of our observed recombination events. While there are portions of the graph where the principal quantum number fluctuates wildly, we also observe a plateau in

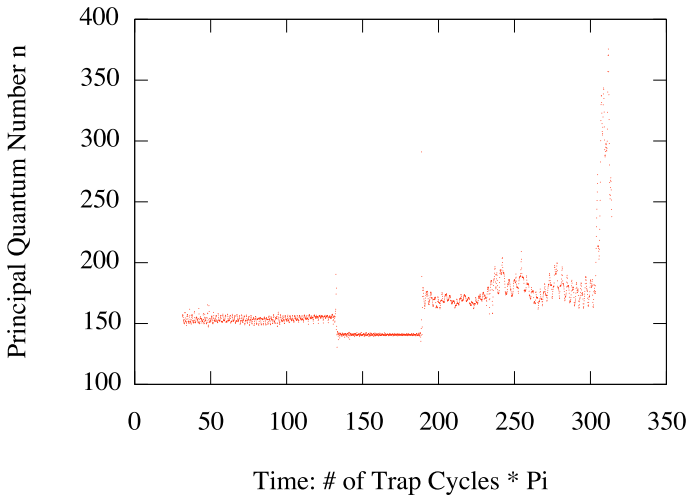

FIG. 2: Principal quantum number $n(t)$ as a function of time for one of our recombination events. A plateau in $n(t)$ is clearly visible.

$n(t)$ of about 30 ns duration, which corresponds to transient $\bar{\mathrm{H}}$ formation in a highly excited Rydberg state.

V. CONCLUSIONS AND OUTLOOK

In this paper we present two fundamentally new and important results. Firstly, our simulations prove that antiprotons and positrons can be simultaneously confined in a Paul trap, due to Coulomb interactions. This is important, because a Paul trap optimized for the storage of positrons is not, by itself, capable of storing antiprotons due to the large mass difference between the two particle species. Secondly, our simulations show that the Paul trap is indeed a viable candidate for synthesizing $\bar{\mathrm{H}}$. While the formed anti-atoms are subsequently destroyed by positron-$\bar{\mathrm{H}}$ collisions, we conjecture that the lifetime of $\bar{\mathrm{H}}$ atoms formed in the Paul trap may be increased greatly by accounting for radiative decay into lower-n states, which results in more strongly bound $\bar{\mathrm{H}}$ atoms that are less susceptible to destruction by collision with positrons.

Looking towards the future, we note that the Paul trap may be able to produce $\bar{\mathrm{H}}$ atoms, but it is not capable of storing them. Therefore, the produced $\bar{\mathrm{H}}$ atoms have to be guided out of the Paul trap and stored in a suitable neutral-particle trap. Several different trap designs are available for achieving this goal; we present the following possibility.

Recent experiments have shown that it is possible to trap neutral atoms in the vortex formed by a (Type-II) superconducting microstructure in its mixed state [19, 20]. We hypothesize that $\bar{\mathrm{H}}$ should be no exception. These vortex traps are presently pursued with atom-optical systems in mind: they open new frontiers for atom optics [19, 20], perhaps in just the way necessary to move forward with $\bar{\mathrm{H}}$ experimentation. This type of trapping procedure would allow us to cool the $\bar{\mathrm{H}}$ even further via Doppler cooling and obtain a direct optical confirmation of the anti-atoms via the scattered light. The difficulty will be in transitioning to the vortex trap from the Paul trap. However, it may be possible that the same magnetic field used to create the Abrikosov vortex could shuttle high-field seeking $\bar{\mathrm{H}}$ out of the Paul trap and into the vortex trap. Preliminary experiments with hydrogen atoms (more practical, at present, than experiments with $\bar{\mathrm{H}}$) may be preformed to explore the prospects of trapping antihydrogen in Abrikosov vortices.

VI. ACKNOWLEDGEMENT

Guy Geyer would like to thank the Wesleyan University Physics Department as well as the American Physical Society Committee on Minorities in Physics for generous grants to support his undergraduate research in the summer of 2010.

---

[1] R. G. Lerner and G. L. Trigg, *Encyclopedia of Physics*, 2nd edition (VCH Publishers, New York, 1991).

[2] P. Morrison, Am. J. Phys. **26**, 358 (1958).

[3] L. I. Schiff, Phys. Rev. Lett. **1**, 254 (1958).

[4] M. Villata, Europhys. Lett. **94**, 20001 (2011).

[5] A. Kellerbauer *et al.* Nucl. Instrum. Meth. B **266**, 351 (2008).

[6] E. F. Taylor and J. A. Wheeler, *Spacetime Physics*, 2nd edition (Freeman, New York, 1992).

[7] G. B. Andresen *et al.*, J. Phys. B: Atomic, Molecular and Optical Physics **41**, 011001 (2008).

[8] G. Gabrielse *et al.*, Phys. Rev. Lett. **89**, 2 (2002).

[9] G. Gabrielse *et al.*, Phys. Rev. Lett. **100**, 1 (2008).

[10] G. B. Andresen *et al.*, Nature Physics **7**, 558 (2011).

[11] W. Paul, Rev. Mod. Phys. **62**, 531 (1990).

[12] R. Blümel, J. M. Chen, E. Peik, W. Quint, W. Schleich, Y. R. Shen, and H. Walther, Nature **334**, 309 (1988).

[13] J. Hoffnagle, R. G. DeVoe, L. Reyna, and R. G. Brewer, Phys. Rev. Lett. **61**, 255 (1988).

[14] D. J. Griffiths, *Introduction to Electrodynamics*, 3rd edition (Prentice Hall, Upper Saddle River, 1999).

[15] Abramowitz M and Stegun I A 1964 *Handbook of Mathematical Functions* (Washington DC: National Bureau of Standards) p 722

[16] H. G. Dehmelt, Adv. Atom. Mol. Phys. **3**, 53 (1967).

[17] W. H. Press, S. A. Teukolsky, W. T. Vetterling, and B. P. Flannery, *Numerical Recipies in Fortran*, 2nd edition (Cambridge University Press, Cambridge, 1996).

[18] J. B. Marion and S. T. Thornton, *Classical Dynamics of Particles and Systems*, 4th edition (Harcourt Brace, Fort Worth, 1995).

[19] B. Zhang, R. Fermani, T. Müller, M. J. Lim, and R. Dumke, Phys. Rev. A **81**, 063408 (2010).

[20] F. Shimizu, C. Hufnagel, and T. Mukai, Phys. Rev. Lett. **103** 253002 (2009).